RSC Advances

PAPER

View Article Online
View Journal | View Issue

Cite this: *RSC Adv.*, 2014, **4**, 30118

Soft hydrogels from tetra-functional PEGs using UV-induced thiol–ene coupling chemistry: a structure-to-property study†

Kristina Olofsson, Michael Malkoch and Anders Hult*

Received 9th May 2014
Accepted 26th June 2014

DOI: 10.1039/c4ra04335a

www.rsc.org/advances

In this work, photo-induced thiol–ene coupling (TEC) was used to produce well-defined poly(ethylene glycol) (PEG)-based hydrogels. PEGs of four different molecular weights (2k, 6k, 10k, and 20k) were functionalized with G1-allyl dendrons using anhydride chemistry to produce tetra-functional TEC crosslinkable PEGs. The tetra-functional PEGs were subsequently crosslinked with a tri-functional thiol in ethanol to form hydrogels. The synthesized hydrogels were characterized with respect to swelling behaviour, rheological properties and hydrolytic degradation. It was found that the molecular weight of the PEG chain greatly influences the final properties of the hydrogel, where a higher molecular weight of PEG gives an increased weight swelling ratio from 240% for PEG-2k hydrogels to 1400% for PEG-20k hydrogels, as well as decreased elastic moduli, with Young's moduli ranging from 106 MPa to 6 MPa, for PEG-2k and PEG-20k hydrogels, respectively. It was also found that the hydrolytic stability in alkaline conditions (pH 10) decreased when the molecular weight of PEG in the hydrogels increased.

Introduction

Hydrogels have attracted much attention for a variety of applications, including anti-fouling coatings, super absorbents, contact lenses, and drug delivery. Due to their high water content, hydrogels are of interest for many biomedical applications such as regenerative medicine, tissue engineering and drug delivery.[1–3] For these applications, good control over the chemical structure of the material is necessary, as well as adequate knowledge about structure–property relationships.

One material that has gained interest in this area is poly(ethylene glycol) (PEG) hydrogels. PEG is a non-toxic, biocompatible polymer, and PEG-based hydrogels have shown great promise in the biomedical field.[1–5] The properties of hydrogels can be tuned by varying the composition of the network and the conditions under which it is formed. The properties can additionally be modified by functionalization of pendant functional groups in the polymer or through copolymerization. As an example, introduction of the peptide sequence Arg-Gly-Asp (RGD) has been successful in promoting cell adhesion to otherwise inert PEG hydrogels,[6] and it has also been shown that incorporation of cleavable moieties in the structure can be used to tune the degradation behaviour.[7]

PEG hydrogels have traditionally been formed through free-radical chain-growth polymerization of PEG with *e.g.* acrylic or methacrylic end-functionalities, where the polymerization of monomers that have more than one functional group leads to network formation. However, in chain-growth polymerization, high molecular weight polymers are formed at low monomer conversions, leading to early gelation. This furthermore leads to restricted movement of monomers through the gel, which can result in inhomogeneous regions in the structure of the resulting network.

Better control over the network structure can be achieved through step-growth polymerization using precursors with a narrow molecular weight distribution. Step-growth polymerization thus enables the formation of hydrogels that are more homogeneous in their structure compared to networks formed using traditional chain-growth mechanisms.[8] Using orthogonal crosslinking chemistries, such as the copper-catalyzed azide–alkyne cycloaddition (CuAAC) or thiol–ene coupling (TEC), enables an even higher level of structural control over the network.[9]

TEC follows a radical-mediated step-growth mechanism that can proceed under mild reaction conditions in various solvents, as well as in the presence of oxygen, with a low level of side reactions.[10,11] It has previously been successfully utilized in the formation of PEG-based hydrogels of linear allyl-functional PEG, where the TEC-crosslinking strategy was utilized as a powerful tool to design traditional hydrogels as well as interpenetrating networks (IPNs) with tunable mechanical properties and swelling behaviour.[12–14] Also, TEC has been used in the crosslinking of norbornene-functionalized PEG with cysteine-

KTH Royal Institute of Technology, Department of Fibre and Polymer Technology, Teknikringen 56-58, SE-100 44 Stockholm, Sweden. E-mail: andult@kth.se; Fax: +46 8 790 8283; Tel: +46 8 790 8268

† Electronic supplementary information (ESI) available. See DOI: 10.1039/c4ra04335a

containing peptides. Hydrogels of this type have *e.g.* been investigated as scaffolds for culturing nerve cells[15] and as biodegradable gels for enzyme-responsive protein delivery to inflammation sites.[16] Additionally, TEC has been successful in the accelerated synthesis of dendrimers[17] and utilized in the formation of bioactive functional hydrogels from linear dendritic hybrids of PEG and bis-MPA-based bi-functional dendrimers.[18] The highly branched and exact structure of dendrimers offers new possibilities in the formation of functional hydrogels and advanced 3D networks.[19]

The aim of this study was to combine TEC with basic dendrimer chemistry in order to gain a better understanding of how the properties of well-defined first-generation allyl-functional PEG hydrogels depend on the structure of the network. Hydrogels with a high level of structural control were synthesized from first-generation tetra-functional PEGs *via* photoinitiated TEC. The swelling and mechanical properties of these hydrogels were assessed and related to the network structure. Additionally, degradation of the hydrogels in aqueous solutions with different pH values was evaluated.

Experimental

Materials

All chemicals were purchased from Sigma-Aldrich and used as received, unless otherwise stated.

2,2-Bis(methylol)propionic acid (Bis-MPA) was kindly supplied by Perstorp Holding AB, Sweden. HCl, $MgSO_4$, and *N*,*N*′-dicyclohexylcarbodiimide (DCC) were purchased from Acros Organics, Fisher Scientific. Pyridine and ethanol (96%) were purchased from VWR. The UV initiator Irgacure 2959 (I2959) was purchased from Ciba Speciality Chemicals, Inc. and pH buffer solutions with pH 4, 7, and 10 were purchased from Scharlau. Deuturated chloroform ($CDCl_3$) for NMR analyses was purchased from Cambridge Isotope Laboratories, Inc. Poly(ethylene glycol) (PEG) with molecular weights of 2 kDa, 6 kDa, 10 kDa and 20 kDa were purchased from Sigma-Aldrich and freeze-dried or stripped with toluene before use.

Instrumentation

Nuclear magnetic resonance (NMR) spectroscopy was attained on a Bruker Avance 400 MHz instrument. ^{1}H NMR spectra were acquired at 400 MHz and ^{13}C NMR spectra were acquired at 100 MHz. $CDCl_3$ was used as solvent, unless otherwise stated, and the residual solvent peak was used as internal standard.

Raman spectra were acquired on a Perkin-Elmer Spectrum 2000 NIR-Raman and obtained data was analysed using Spectrum software. All spectra were based on 32 scans and acquired using a laser power of 800–1500 mW.

Size exclusion chromatography (SEC) was performed on a TOSOH EcoSEC HLC-8320GPC system from PSS GmbH equipped with an EcoSEC RI detector and three columns: PSS PFG 5 μm; Microguard, 100 Å; and Microguard 300 Å (MW resolving range: 100–300 000 g mol^{-1}). DMF (0.2 mL min^{-1}) with 0.01 M LiBr was used as the mobile phase at 50 °C. A conventional calibration method was created using PEG standards. Toluene was used as an internal standard to correct for flow rate fluctuations and PSS WinGPC Unity software (version 7.2) was used to process obtained data.

Differential Scanning Calorimetry (DSC) was carried out on a Mettler Toledo DSC-1 equipped with the Gas Controller GC100. The analyses were run under nitrogen atmosphere (30 mL min^{-1}) at a temperature interval of −65 °C to 150 °C with a heating/cooling rate of 10 °C min^{-1} and 2 min isotherms. STAR^e Excellence Software was used for evaluation of data.

Matrix-assisted laser-desorption ionization - time-of-flight mass spectroscopy (MALDI-ToF MS) was conducted on a Bruker UltraFlex MALDI-ToF MS with a SCOUT-MTP ion source (Bruker Daltonics) equipped with a N_2-laser (337 nm), and a gridless ion source. Acquisition of spectra was done in reflector mode, with the exception of spectra for PEG-20k-OH and PEG-20k-G1-allyl which were acquired in linear mode, and the samples were prepared using using HABA and NaTFA as matrix and counter ion source, respectively. SpheriCal™ calibrants (Polymer Factory Sweden AB) were used to calibrate the instrument and obtained spectra were analyzed using FlexAnalysis (Bruker Daltonics, v. 2.2). Average molecular weights ($\bar{M}_n$) and dispersities ($Đ$) were acquired using Polytools v. 1.0.

Rheology measurements were carried out on hydrogels swollen to equilibrium on an Ares RDA-III rheometer (TA Instruments) at 25 °C using a Ø 25 mm parallel-plate geometry. Dynamic strain sweep tests (0–60% strain, 10 rad s^{-1}) and dynamic frequency sweep tests (0–100 rad s^{-1}, 5% strain) were used to identify the linear region, after which dynamic time sweep tests (5% strain, 10 rad s^{-1}) were used to determine the storage and loss moduli of the hydrogels.

Tensile tests were conducted on an Instron 5944 tensile testing machine equipped with a standard video extensometer. Measurements were done on dog-bone-shaped hydrogels swollen to equilibrium in deionized (DI) water at 23 °C using a cross-head speed of 5 mm min^{-1} and a 500 N load cell.

Synthesis of bis(allyl propionic acid), BAPA

Synthesis of BAPA was accomplished in accordance with a previously published procedure.[17] Bis-MPA (50.00 g, 0.3728 mol) and NaOH (149.1 g, 3.728 mol) were dissolved in toluene (750 mL) and heated to 110 °C. Allyl bromide (225.8 mL, 2.609 mol) was added and the reaction was carried out overnight. The reaction mixture was allowed to reach room temperature and then acidified using concentrated HCl (37%, 150 mL). The product was purified through extraction three times with 250 mL DI water, after which the toluene phase was dried over $MgSO_4$ and the solvent removed under reduced pressure to yield BAPA as a colourless viscous liquid (72.65 g, 0.3391 mol, 90.97% yield). ^{1}H NMR ($CDCl_3$, 400 MHz): 1.24 (s, –CH_3), 3.56 (q, ┼C–CH_2–O–, 4.00 (dd, –O–CH_2–CH═), 5.24 (m, –CH═CH_2), 5.87 (m, –CH═CH_2), 11.33 (br s, –OH). ^{13}C NMR ($CDCl_3$, 100 MHz): 18.06 –CH$_3$), 48.30 (┼C–CH$_3$), 71.93 (–O–CH$_2$–CH═), 72.51 (┼C–CH$_2$–O–), 117.02 (═CH$_2$), 134.72 (–CH═CH$_2$), 180.82 (HOOC–).

Synthesis of bis(allyl propionic acid anhydride), BAPA anhydride

BAPA anhydride **1** was synthesized *via* DCC coupling in accordance with a previously published procedure[20] and conducted as follows; BAPA (71.47 g, 0.3336 mol) was dissolved in 100 mL dichloromethane (DCM) and cooled to 0 °C. DCC (34.41 g, 0.1668 mol), mixed with 10.00 mL DCM, was slowly added to the reaction vessel and the reaction mixture was stirred overnight. By-products were filtered off and the solvent was evaporated under reduced pressure to give BAPA anhydride **1** as a viscous liquid (53.87 g, 0.1312 mol, 78.68% yield). ^{1}H NMR ($CDCl_3$, 400 MHz): δ 1.27 (s, –CH_3), 3.58 (s, ┼C–CH_2–O–), 3.99 (d, –O–CH_2–CH═), 5.24 (m, –CH═CH_2), 5.86 (m, –CH═CH_2). ^{13}C NMR ($CDCl_3$, 100 MHz): δ 17.44 (–CH$_3$), 49.95 (┼C–CH$_3$), 71.54 (–O–CH$_2$–CH═), 72.44 (┼C–CH$_2$–O–), 116.92 (═CH$_2$), 134.65 (–CH═CH$_2$), 169.64 (–OOC–O–COO–).

General procedure for the synthesis of PEG-G1-allyl

PEG-OH with $\bar{M}_n$ = 2 kDa, 6 kDa, 10 kDa, and 20 kDa were dendronized using BAPA anhydride **1** to give PEG-G1-allyl **2**, Scheme 1a. In the following paragraph, the synthesis of PEG-6k-G1-allyl will be described in detail. Detailed information regarding the syntheses of PEG-2k-G1-allyl, PEG-10k-G1-allyl, and PEG-20k-G1-allyl can be found in the ESI.†

Synthesis of PEG-6k-G1-allyl. PEG-OH ($\bar{M}_n$ = 6 kDa) (19.97 g, 3.328 mmol), DMAP (163.0 mg, 1.334 mmol), and pyridine (1.610 mL, 19.99 mmol) were dissolved in 15.00 mL DCM. Using an ice-bath, BAPA anhydride **1** (3.830 g, 9.330 mmol), dissolved in 1.000 mL DCM, was added dropwise and the solution was allowed to react over-night. An additional amount of DMAP (80.0 mg, 0.666 mmol) was added to ensure complete reaction and full conversion of OH-groups was confirmed using ^{13}C NMR analysis. Purification was achieved through precipitation from DCM in diethyl ether 3 times. (16.57 g, 2.593 mmol, 77.89% yield). ^{1}H NMR ($CDCl_3$, 400 MHz): δ 1.22 (s, –CH_3), 3.57 (d, ┼C–CH_2–O–), 3.65 (s, –CH_2– (PEG)), 3.98 (dd, –O–CH_2–CH═), 4.26 (t, PEG–CH_2–OOC–G1), 5.15 (dd, –CH═CH_2 (cis)), 5.25 (dd, –CH═CH_2 (trans)), 5.86 (m, –CH═CH$_2$). ^{13}C NMR ($CDCl_3$, 100 MHz): δ 18.11 (–CH$_3$), 48.56 (┼C–CH$_3$), 63.82 (–PEG–CH$_2$–OOC–G1), 69.29 (–O–CH$_2$–CH$_2$–COO–G1), 70.74 (–CH$_2$– (PEG)), 72.22 (–O–CH$_2$–CH═), 72.41 (┼C–CH$_2$–O–), 116.62 (═CH$_2$), 135.02 (–CH═CH$_2$), 174.70 (PEG–OOC–G1). SEC: $\bar{M}_n$ = 6266 g mol^{-1}, $Đ$ = 1.04.

The same purification protocol was used for PEG-10k-G1-allyl and PEG-20k-G1-allyl, with precipitation in diethyl ether 2–4 times, whereas PEG-2k-G1-allyl was purified through subsequent extraction with $NaHSO_4$ (10%) and $NaHCO_3$ (10%), after which the organic phase was dried over $MgSO_4$, filtered, and the solvent removed under reduced pressure.

General procedure for hydrogel formation

Hydrogels were produced by crosslinking PEG-G1-allyl **2** with trimethylolpropane tris(3-mercaptopropionate) (TMP-(SH)$_3$) using an allyl-to-thiol ratio of 1 : 1 and a solid content of 50 wt% in ethanol (96%), Scheme 1b. The formation of hydrogels from PEG-6k-G1-allyl will here be described in detail. Details regarding the formation of hydrogels from PEG-2k-G1-allyl, PEG-10k-G1-allyl, and PEG-20k-G1-allyl can be found in the ESI.†

Formation of PEG-6k-G1-allyl hydrogels. PEG-6k-G1-allyl (2.000 g, 0.3129 mmol) and TMP-(SH)$_3$ (137.0 μL, 0.4159 mmol) were dissolved in ethanol (96%, 2.758 mL) along with the initiator I2959 (10.9 mg, 0.50 wt% of total solid content). Hydrogels were formed between two glass slides *via* UV irradiation using a Blak-Ray® XX-15BLB UV Bench Lamp (UVP, Cambridge, UK, 365 nm, 28.5 mW cm^{-2}) for 20 min. After

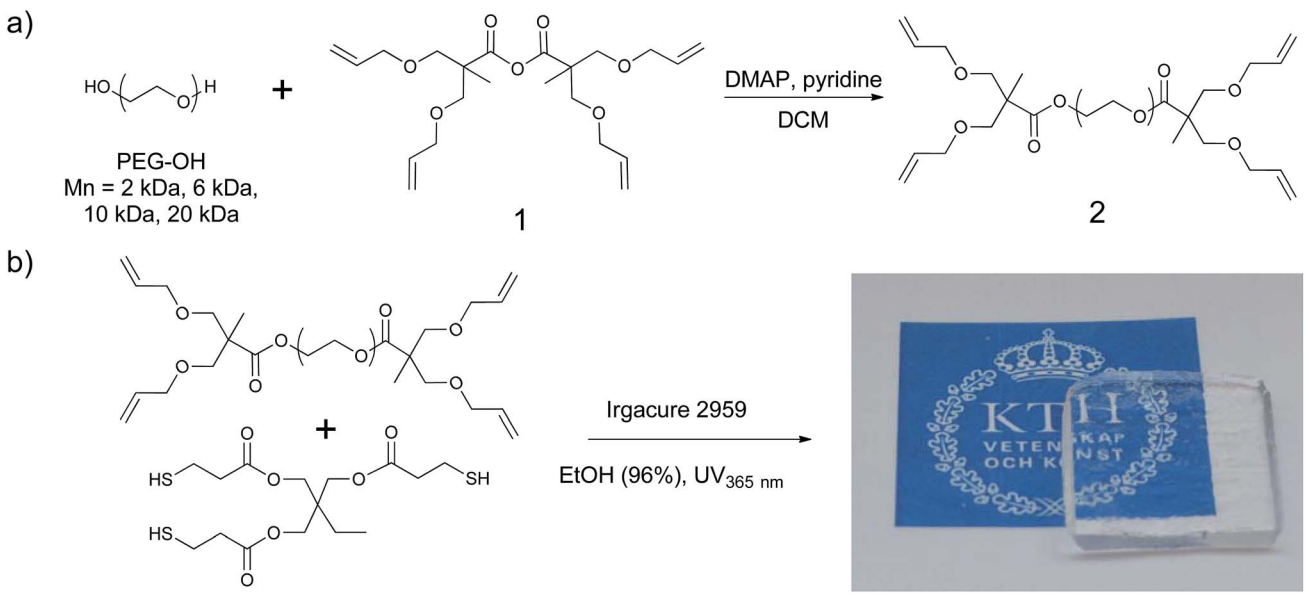

Scheme 1 Synthetic procedures. (a) Synthesis of PEG-G1-allyl **2** *via* functionalization of PEG-OH using BAPA anhydride **1** and (b) hydrogel formation *via* UV-induced TEC.

curing, hydrogels were washed in DI water (overnight + 2 h + 2 h) and subsequently in ethanol (96%, 2 h + 2 h) to remove residual reactants and thereafter the hydrogels were dried in air overnight followed by 12 h in a vacuum oven at 50 °C. The gel fraction (GF) was determined from the differences in dry weight of hydrogels before and after washing according to eqn (1):

$$\mathrm{GF} = \frac{w_{\mathrm{d,washed}}}{w_{\mathrm{d,cured}}} \times 100\% \quad (1)$$

where GF is the gel fraction (%), $w_{\mathrm{d,washed}}$ is the weight of the dried hydrogel after washing (g), and $w_{\mathrm{d,cured}}$ is the weight of the dried hydrogel after curing (g).

Swelling experiments

Swelling experiments in DI water were conducted on thoroughly washed and dried hydrogels at 23 °C. Hydrogels were dried in a vacuum oven at 50 °C before the dry weight of each specimen was measured. The swelling in water was measured at several different swelling times for each specimen. Before weighing, excess water was gently removed from the surface of the hydrogels using a tissue paper. The swelling ratio (SR) was calculated using eqn (2):

$$\mathrm{SR} = \frac{m_{\mathrm{w}} - m_{\mathrm{d}}}{m_{\mathrm{d}}} \quad (2)$$

where SR is the swelling ratio, m_{w} is the weight of the swollen hydrogel (g), and m_{d} is the weight of the dry hydrogel before swelling (g).

Degradation study

Hydrolytic degradation of the hydrogels was studied in buffer solutions from Scharlau with three different pH values, pH 4 (potassium hydrogen phthalate), pH 7 (potassium di-hydrogen phosphate/di-sodium hydrogen phosphate), and pH 10 (sodium carbonate/sodium hydrogen carbonate). Degradation times were estimated from visual inspection and two replicas were used for each hydrogel system. The study was terminated after three months, after which the solutions were freeze-dried and analysed using MALDI-ToF MS and NMR.

Results and discussion

Synthesis of allyl-functional PEGs

PEG-OH ($\bar{M}_{\mathrm{n}}$ = 2000, 6000, 10 000, and 20 000 g mol^{-1}) were functionalized with BAPA anhydride **1** to give PEG-G1-allyl **2** with four allyl groups available for UV-initiated TEC reactions.

The functionalization of PEG-OH was monitored with ^{13}C NMR to ensure complete conversion of the hydroxyl groups. The ^{13}C NMR spectrum for the pure product of PEG-6k-G1-allyl can be seen in Fig. 1b, along with spectra for BAPA anhydride and unmodified PEG-6k-OH. As a result of the functionalization, some characteristic peaks in the spectra changed shift. This was used to monitor all allylation reactions until complete conversion of OH-groups was observed. As can be seen when comparing the spectra in Fig. 1b, the peak corresponding to the methylene carbon in PEG-OH closest to the OH-group changed shift from 61 ppm to 63 ppm upon functionalization with BAPA anhydride. Additionally, the peak in the spectra that corresponds to the carbonyl carbon shifted from 169 ppm for the anhydride to 173 ppm for the formed ester in PEG-6k-G1-allyl. The chemical shifts for the other peaks were also in accordance with expected values, as were the chemical shifts in the ^{1}H NMR spectra in Fig. 1a.

SEC was used to verify the functionalization and to determine the number average molecular weights ($\bar{M}_{\mathrm{n}}$) of functionalized as well as unmodified PEG materials. In Fig. 2a, an increase in molecular weight can be seen between unmodified and modified PEG, verifying the functionalization. The dispersities calculated from SEC were narrow for all materials with values below 1.06. The obtained molecular weights, which can be found in Table 1, were found to correlate reasonably well with the expected values.

For both PEG-20k-OH and PEG-20k-G1-allyl, a broadening of the signals from SEC could be seen, Fig. 2a. That this broadening effect could be seen for both modified and unmodified PEG20k, suggested that it was an artefact from the starting material and not an effect of the functionalization.

Successful functionalization of PEG-OH to PEG-G1-allyl was also confirmed by MALDI-ToF MS, Fig. 2b. If the 2k system is studied as an example, it can be seen that the distance between the two populations in the two spectra is 392.5 m/z, which corresponds to the substitution of both hydroxyl end groups to G1-allyl. Furthermore, as SEC results suggested, two populations with different molecular weights can be seen for both modified and unmodified PEG-20k. A closer look confirms complete functionalization and the bimodal nature of the samples is thus an artefact from the original synthesis of PEG-20k-OH.

Thermal properties

The thermal properties of synthesized materials were assessed using differential scanning chromatography (DSC). Results from DSC in Fig. 3 show that the temperatures for crystallization and melting, as well as the degree of crystallinity, are reduced when PEG-OH is modified into PEG-G1-allyl. This can be explained by a reduced ability to form hydrogen bonds between the polymer chains and also that the G1-allyl end groups introduce more free volume in the materials. It should be noted that the melting enthalpy for 100% crystalline PEG-OH has been used for the calculations of the degree of crystallinity for both modified and unmodified PEGs. The values for the degree of crystallinity for the modified PEG materials should thus only serve as an indication and not be considered to be absolute values. It is however clear that an increased chain length of PEG-G1-allyl increases the transition temperatures of melting and crystallization, as well as the degree of crystallinity. The influence of the functionalization, *i.e.* the differences between PEG-OH and PEG-G1-allyl, is less apparent when the PEG chain becomes longer, probably because the influence of the chain ends is less prominent when the chain length increases. The crystallization temperature was *e.g.* lowered by 9 degrees (from 27 °C to 18 °C) for the 2k system, while the decrease in crystallization temperature for the 20k system was

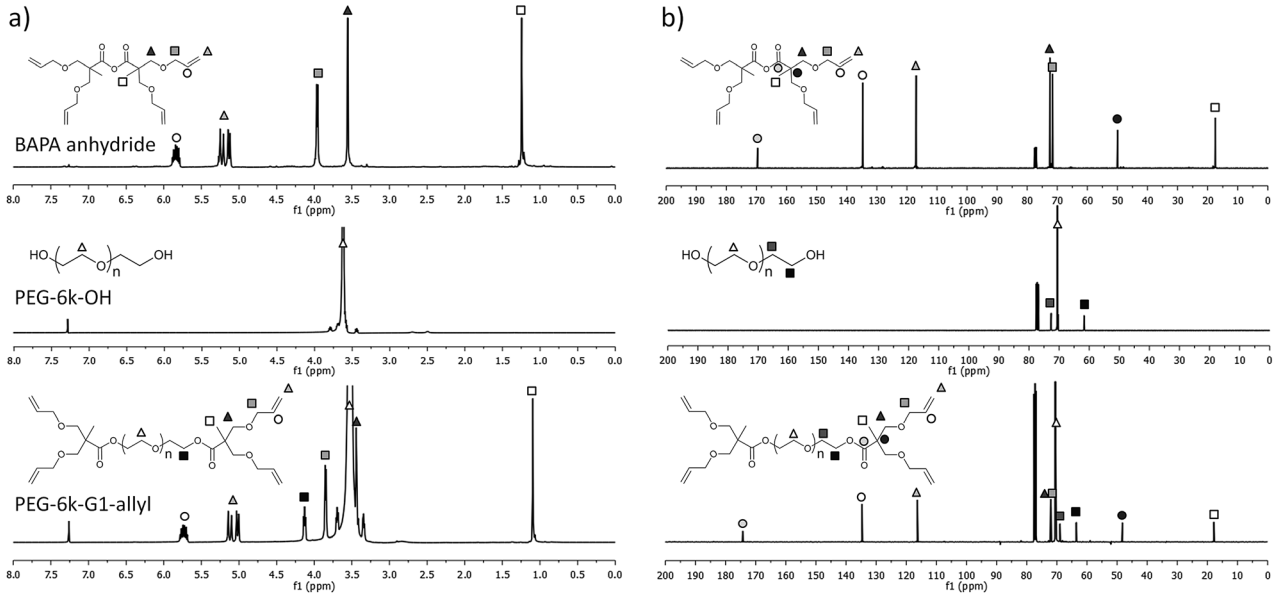

Fig. 1 (a) ^{1}H NMR spectra and (b) ^{13}C NMR spectra of BAPA anhydride **1**, unfunctionalized PEG-6k-OH, and synthesized PEG-6k-G1-allyl **2**. The residual solvent peak of $CDCl_3$ was used as internal reference.

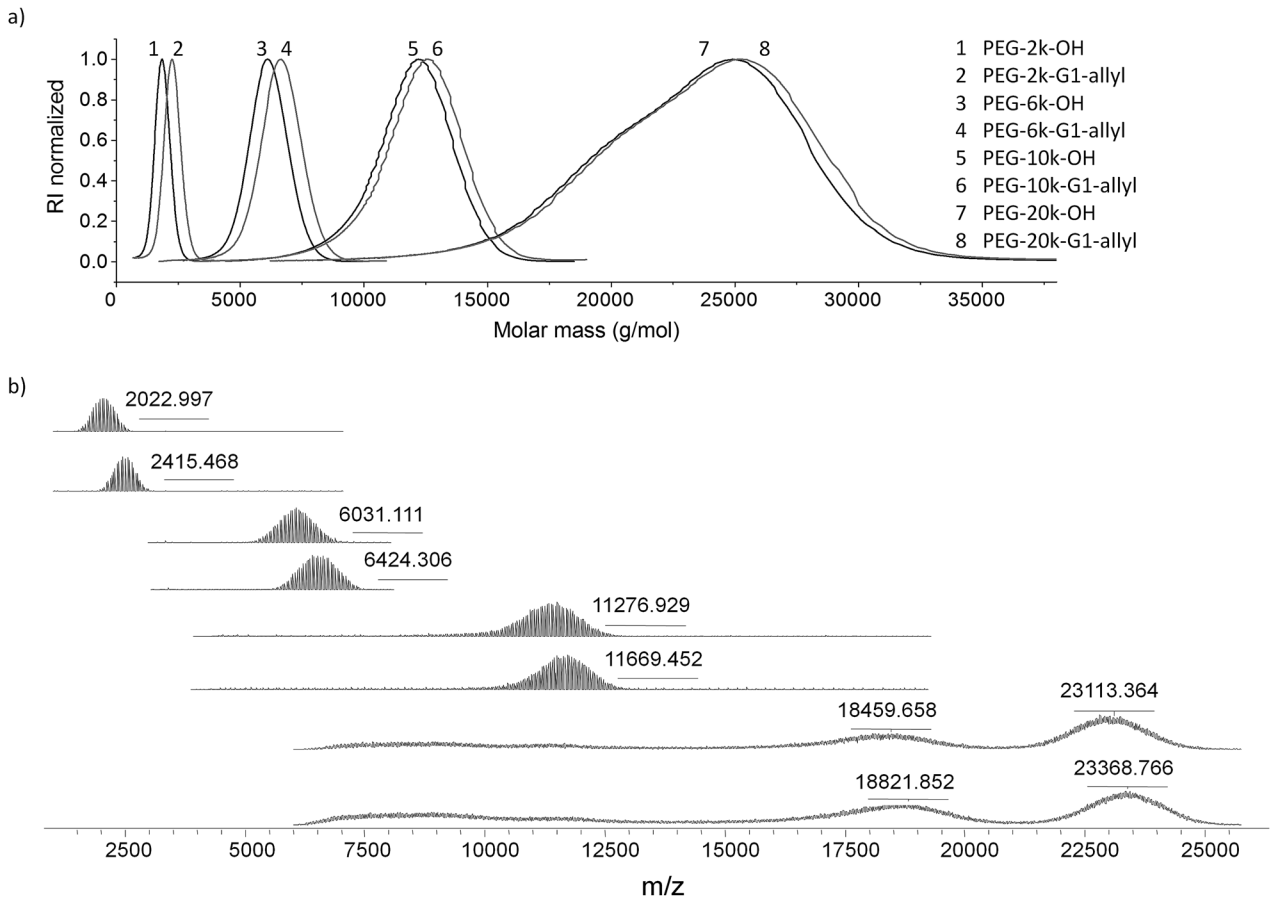

Fig. 2 (a) Molecular weights for all functionalized and unfunctionalized PEG materials obtained by SEC in DMF calibrated against PEG standards. (b) MALDI-ToF spectra for all modified and unmodified PEGs. Spectra for PEG-20k and PEG-20k-G1-allyl were acquired in linear mode.

Table 1 Comparison of theoretical and measured molecular weights and dispersities obtained from SEC and MALDI-ToF MS for unmodified and modified PEG materials. (All molecular weights are reported in g mol^{-1}.)

Sample	$M_{n,th}$	M_n [a]	Đ [a]	M_n [b]
PEG-2k	2000	1727	1.04	2004
PEG-2k-G1-allyl	2393	2147	1.03	2434
PEG-6k	6000	5862	1.02	6059
PEG-6k-G1-allyl	6393	6266	1.04	6426
PEG-10k	10 000	11 278	1.03	11 047
PEG-10k-G1-allyl	10 393	11 571	1.03	11 573
PEG-20k	20 000	21 676	1.05	—
PEG-20k-G1-allyl	20 393	21 915	1.06	—

[a] Values obtained from DMF-SEC using PEG standards. [b] Values obtained from MALDI-ToF MS data using Polytools software. No values could be obtained for PEG-20k and PEG-20k-G1-allyl due to poor resolution of the spectra.

only 0.8 degrees (from 44.6 °C to 43.8 °C). There were even larger differences in the melting temperatures, where the functionalization caused a decrease in melting temperature with 21 degrees for the 2k system and 5 degrees for the 20k system.

Hydrogel formation

Hydrogels of PEG-G1-allyl and TMP-$(SH)_3$ were successfully formed under irradiation with UV light. The hydrogels had a uniform appearance without visible defects and a gel fraction (GF) above 90% (96 ± 4%, 91 ± 1%, and 90 ± 1% for hydrogels of PEG-6k-G1-allyl, PEG-10k-G1-allyl, and PEG-20k-G1-allyl, respectively), with the exception of hydrogels made from PEG-2k-G1-allyl, where the GF was 79 ± 9%. The lower GF for the PEG-2k-G1-allyl hydrogels indicated that the curing process was not as effective for crosslinking PEG-2k-G1-allyl as for the longer PEGs. This could be due to the relatively lower initiator-to-monomer ratio, leaving more functional groups unreacted during the curing process in comparison with the other hydrogel systems.

In order to determine if there were unreacted allyl or thiol groups left in the hydrogels after curing, unwashed hydrogels were studied using RAMAN spectroscopy. The RAMAN spectra shown in Fig. 4 suggest that all hydrogels, including hydrogels from PEG-2k-G1-allyl, were fully cured, as no traces of allyl or thiol could be seen in the spectra, at 1730 and 2573 cm^{-1}, respectively. (The peak seen at 1734 cm^{-1} for TMP-$(SH)_3$ corresponds to the C=O stretch of the carbonyls in the structure of the crosslinker.) Effective curing, in combination with high gel content, thus showed that UV-induced TEC was a robust strategy for hydrogel formation.

Swelling properties

The high water content of hydrogels is one of the main properties of interest for many biomedical applications. In accordance with theory, there is a strong correlation between the swelling properties and the chain length between crosslinks.[21] The kinetic swelling study conducted in this work is summarized in Fig. 5a and shows that the equilibrium swelling increases with the length of the hydrophilic PEG chain, from 240% to 1400% for hydrogels based on PEG-2k-G1-allyl and PEG-20k-G1-allyl, respectively, as seen in Fig. 5b and Table 2. These swelling ratios are lower than swelling ratios obtained for similar hydrogel systems from linear di-functional PEG-allyl with the same molecular weights, where the swelling for 2k and 6k hydrogels were found to be 380% and 750%,[13] as compared to 240% and 650%, which were obtained for 2k and 6k hydrogels in this study. This difference is to be expected due to the higher number of functional groups of the tetra-functional PEG-G1-allyls herein presented. For hydrogels with the same molecular weight of PEG, more of the lower molecular weight crosslinker, TMP-$(SH)_3$, had to be added to the tetra-functional PEGs in order to keep the allyl-to-thiol ratio at 1 : 1 in the hydrogels. This thus resulted in a tighter network compared to the di-functional PEGs, and thereby lower swelling ratios. Additionally, it can be seen in Fig. 5a that hydrogels with shorter PEG chains reach their equilibrium swelling ratio faster than hydrogels with longer chain segments.

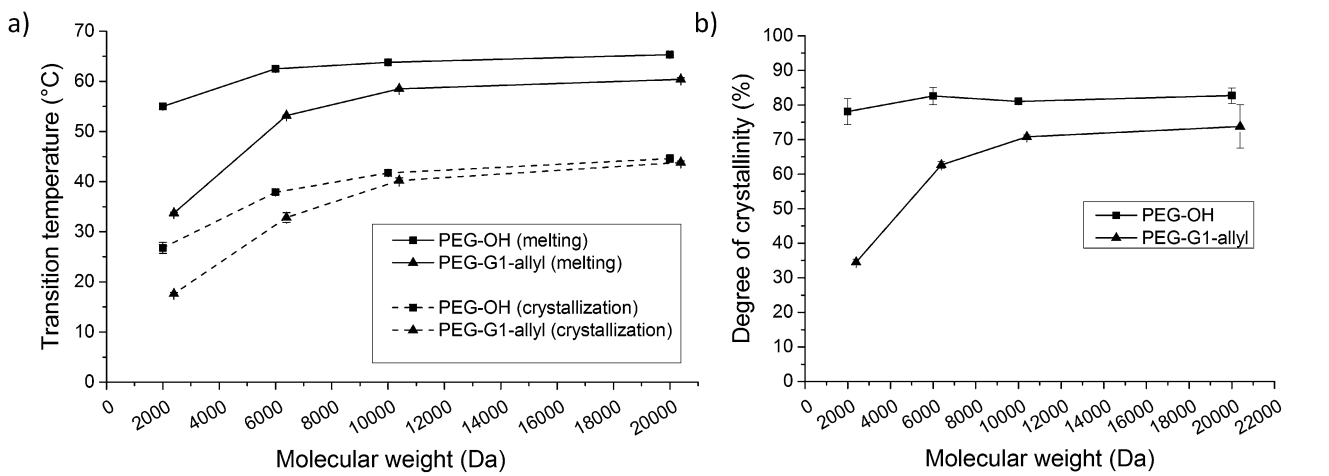

Fig. 3 Thermal properties of modified and unmodified PEG materials obtained from DSC. (a) Transition temperatures for melting and crystallization. (b) Degree of crystallinity. (Calculated from the enthalpy of melting during the second heating.)

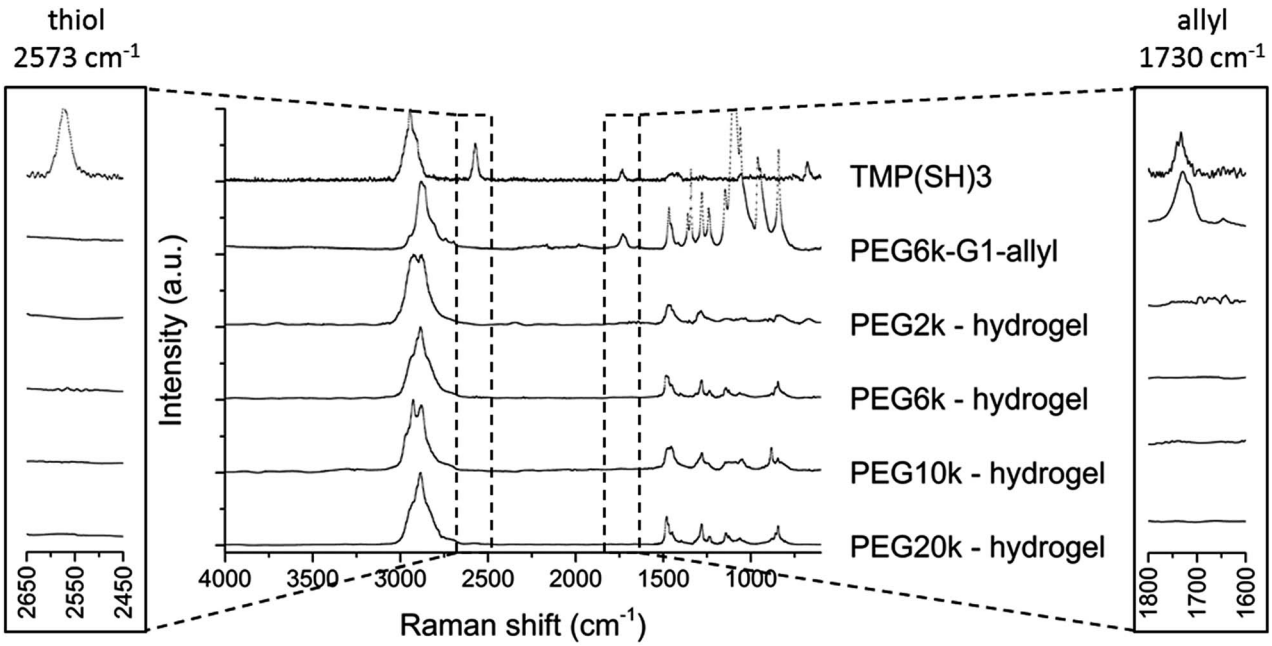

Fig. 4 RAMAN spectra of unwashed hydrogels after curing, showing no signs of residual allyl or thiol functional groups.

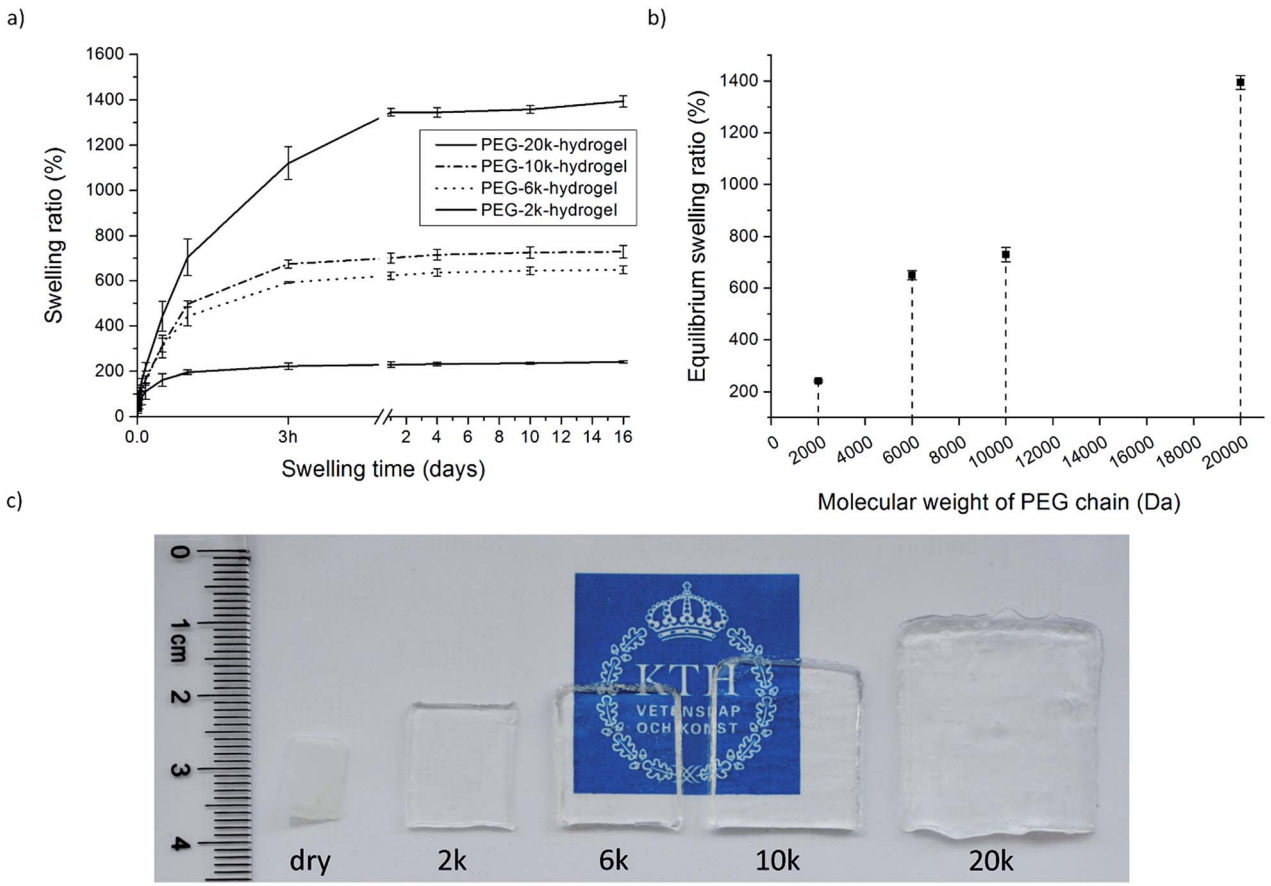

Fig. 5 (a) Swelling ratio as a function of swelling time for hydrogels swollen in deionized water at 23 °C and (b) equilibrium swelling ratio as a function of molecular weight of the PEG chain in the hydrogel. (c) Photograph of hydrogels swollen to equilibrium in DI water at 23 °C.

Table 2 Swelling ratio (SR), and mechanical properties, for hydrogels of PEG-G1-allyl crosslinked with TMP-$(SH)_3$

PEG MW (g mol^{-1})	SR (%)	G' (kPa)	G'' (kPa)	tan δ	E^a (kPa)
2000	241 ± 5	35.4 ± 4.4	19.5 ± 4.7	0.55 ± 0.15	106 ± 13
6000	649 ± 17	20.7 ± 3.6	13.4 ± 3.0	0.65 ± 0.18	62 ± 11
10 000	730 ± 28	13.4 ± 0.7	6.7 ± 3.3	0.50 ± 0.25	40 ± 2
20 000	1390 ± 26	1.98 ± 0.11	0.37 ± 0.18	0.19 ± 0.09	5.9 ± 0.3

[a] Young's moduli calculated from the storage moduli (G') obtained from rheology measurements using eqn (4).

Hydrogels made from PEG-2k-G1-allyl are close to equilibrium swelling after just three hours, whereas the swelling of hydrogels made from PEG-6k-G1-allyl, PEG-10k-G1-allyl, and PEG-20k-G1-allyl stagnates after approximately 24 hours. It should also be noted that the swelling kinetics are greatly affected by the drying conditions. Freeze-dried hydrogel samples *e.g.* have a porous structure where capillary forces give rise to an increased water absorption rate compared to that of the vacuum dried samples tested in this study, for which the main driving force of absorption is diffusion.

As can be seen from the swelling experiment, there are large differences in water absorption for the different hydrogels. Fig. 5c shows a photograph of the swollen hydrogels, where significant differences between the systems can be seen. Changing the molecular weight of the PEG-G1-allyl that makes up the main part of the hydrogel network can thereby be used as a means to easily tune the swelling properties for a certain application.

The obtained equilibrium swelling was moreover used to calculate the average molecular weight between crosslinks ($\bar{M}_c$) for the synthesized hydrogels. Calculations of $\bar{M}_c$ were made using the Peppas–Merrill model,[22] which is derived from the equation originally introduced by Flory,[23] according to eqn (3):

$$\overline{M}_c = -\frac{\rho_p V_1 \left[\left(\frac{\nu_{2,s}}{\nu_{2,r}} \right)^{1/3} - \frac{1}{2} \left(\frac{\nu_{2,s}}{\nu_{2,r}} \right) \right]}{\ln(1-\nu_{2,s}) + \nu_{2,s} + \chi(\nu_{2,s})^2} \quad (3)$$

where ρ_p is the polymer density (1.125 g cm^{-3} for PEG[24]), V_1 is the molar volume of the solvent (18 cm^3 mol^{-1} for water), $\nu_{2,s}$ is the volume fraction of polymer in the swollen gel, $\nu_{2,r}$ is the volume fraction of polymer in the relaxed gel during gel formation, and χ is the Flory polymer–solvent interaction parameter (0.426 for PEG–water[25]) For further details, please see the ESI.†

The obtained values of $\bar{M}_c$ were 333, 2520, 3640, and 10 830 g mol^{-1} for hydrogels based on PEG-2k-G1-allyl, PEG-6k-G1-allyl, PEG-10k-G1-allyl, and PEG-20k-G1-allyl, respectively. The obtained $\bar{M}_c$ was found to be much lower than expected for all hydrogel systems. One explanation for this can be that $\bar{M}_c$ is measured between kinetically active crosslinks and not only between covalent crosslinking points. In all probability, the relatively high solid content during gel formation in this study (50 wt%) meant that the polymer chains were intertwined in the solution during crosslinking, giving rise to physical entanglements in the final network structure.[26–28] These entanglements can act as kinetically active crosslinks, and as a result, $\bar{M}_c$ values will be lower than expected.

Elastic properties

Mechanical analyses of the hydrogels were conducted using tensile tests and rheology. Tensile tests revealed that the hydrogels had elastic characteristics with strains at break around 23–30%, where hydrogels based on PEG-2k-G1-allyl displayed the highest strain at break with 30 ± 4%. Due to large standard deviations, there were no significant differences in the measured strains at break for hydrogels based on PEG-2k-G1-allyl. PEG-6k-G1-allyl, and PEG-10k-G1-allyl. Hydrogels based on PEG-10k-G1-allyl did however display a measurably lower stress at break and tensile toughness than hydrogels based on PEG-2k-G1-allyl and PEG-6k-G1-allyl. Hydrogels based on PEG-20k-G1-allyl could unfortunately not be evaluated using tensile tests, since the samples broke under their own weight during clamping in the machine due to the high water content. Please see Table S2 in the ESI for further details.†

Due to large variations in the data obtained during tensile tests, rheology was found to be a more suitable method for analysing the mechanical properties of the hydrogels. Rheology measurements were conducted on fully swollen circular hydrogel samples using parallel-plate geometry. The storage modulus (G') and the loss modulus (G'') were determined using a dynamic time sweep test at 5% strain with a frequency of 10 rad s^{-1}. For each hydrogel system, a minimum of 5 replicas were used.

The results from rheology shown in Fig. 6 reveal that less dense hydrogels are more ductile than hydrogels with shorter chain segments between crosslinks, which is in accordance with values that have been previously reported.[12,18] There is also a tendency towards larger differences between storage and loss moduli for hydrogels that are more densely crosslinked. This implies that the viscous part of the material properties increases as the hydrogels become less crosslinked and the water content increases.

For all tested hydrogels, G' was found to be higher than G''. Therefore, G' was estimated to be equal to the shear modulus (G) which could then be used to calculate the Young's moduli (E) for the hydrogels according to rubber elasticity theory using eqn (4):

$$E = 2G(1+\nu) \quad (4)$$

where E is the Young's modulus (Pa), G is the shear modulus (Pa) and ν is Poisson's ratio. The calculations were made assuming a Poisson's ratio of 0.5. The calculated Young's moduli, which can be found in Table 2, range from 6 to 106 kPa,

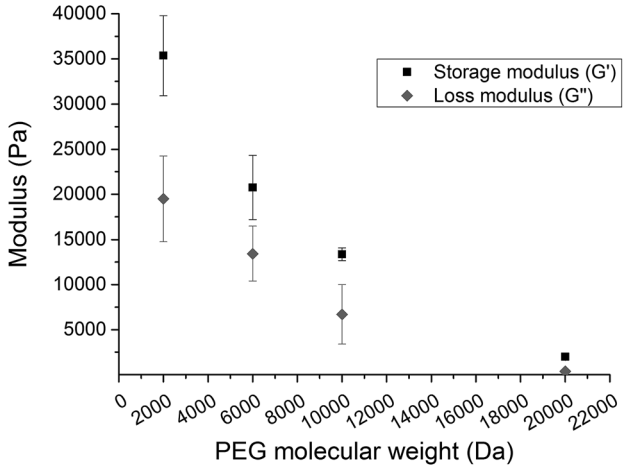

Fig. 6 Storage and loss moduli of formed hydrogels acquired from rheology (time sweep measurements with 5% strain at 10 rad s^{-1}). All measurements were conducted on hydrogels swollen to equilibrium.

depending on the chain length of PEG-G1-allyl. These values are in the same range as several soft body tissues[29] and also in the same range as earlier published results for similar hydrogels.[18,30]

Additionally, the loss factor, tan δ, was significantly lower for PEG-20k-G1-allyl hydrogels than for the other hydrogels, indicating that the viscous characteristics of the 20k hydrogels were more pronounced than for the other hydrogel systems. This is probably an effect of the large quantities of water in the PEG-20k-G1 hydrogels.

Hydrolytic degradation

Hydrolytic degradation of the hydrogels was studied in buffer solutions at three different pH values: pH 4, pH 7, and pH 10. Visual inspection was used to assess the degradation and the time from immersion until complete dissolution of the hydrogels was noted. Undissolved samples were continuously investigated throughout the study using tweezers in order to detect large changes in mechanical stability. No large changes could be discerned for the undissolved samples.

It is known that the hydrolysis of ester bonds can be base catalysed[31] and it was therefore hypothesized that degradation would be faster at pH 10 than at pH 4 and 7. Visible signs of degradation could not be detected in buffer solutions of pH 4 and pH 7 during the three months the degradation study was carried out. However, signs of degradation could be seen already after 48 h in buffer solution with pH 10. As shown in

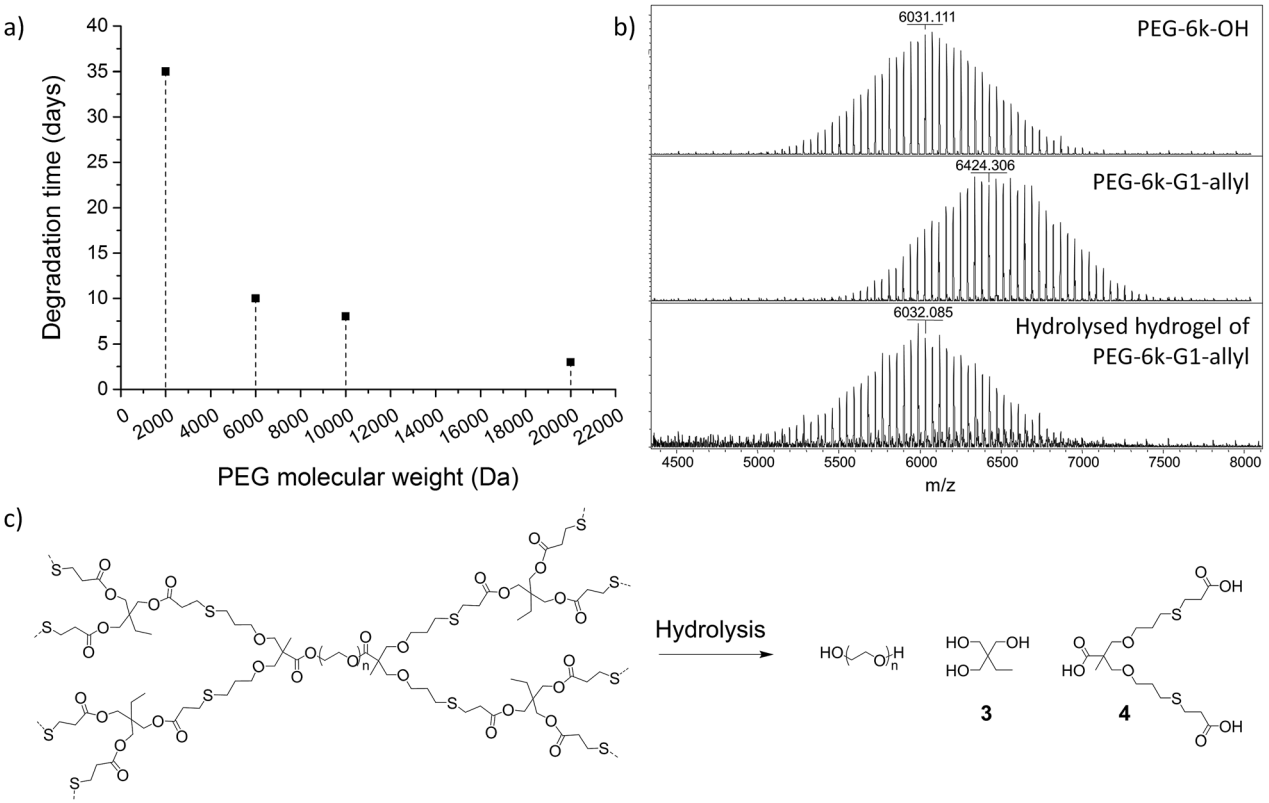

Fig. 7 (a) Degradation time (days) for hydrogels hydrolysed in pH 10 buffer solution, time until complete dissolution into the medium assessed *via* visual inspection. (b) MALDI-ToF MS of freeze-dried samples of PEG-6k-G1-allyl and the PEG-6k-hydrogel after degradation in pH 10 buffer solution for three months. On top is a mass spectrum of unmodified PEG-6k-OH for comparison. (c) Potential degradation products after hydrolysis of the ester bonds in the hydrogels, PEG-OH, TMP **3**, and compound **4** (9-methyl-7,11-dioxa-3,15-dithiaheptadecane-1,9,17-tricarboxylic acid). Degradation products from uncured thiol compounds that might be present in the hydrogels have not been taken into account.

Fig. 7a, PEG-20k-hydrogels were completely dissolved after 3 days, whereas PEG-6k and PEG-10k hydrogels were dissolved after 8 and 10 days, respectively, while PEG-2k hydrogels were stable for 5 weeks. A previous study regarding the hydrolytic degradation of bis-MPA based dendrimers confirms that hydrolytic degradation is faster at alkaline pH.[32] The study showed degradation of the ester bonds in a generation four dendrimer already after six hours in aqueous solution with pH 7.5 at 37 °C. In the same study, it was also shown that the hydrolysis rate was slower at lower temperatures and that the bis-MPA based dendrimer was stable for three weeks when subjected to a solution with pH 7.5 at 8 °C. With those results in mind, it was interesting to notice that there were no visible signs of degradation of the hydrogels synthesized in this study in buffer solutions of pH 7 at 23 °C after three months. An explanation for this can be that the ester bonds are more shielded in the crosslinked hydrogels than they are in a dendrimer.

The degradation study clearly showed that the degradation rate in aqueous buffer at pH 10 depends of the chain length of the PEG. A reason for this can be that hydrogels made from longer PEG chains also exhibit a higher swelling degree, thereby exposing the ester bonds inside the structure to the alkaline solution. The hydrogels with longer chains between crosslinks also contain a much lower relative amount of crosslinks in the structure, and therefore degradation of the ester bonds results in degradation of the crosslinking points faster for these gels and thereby a more rapid dissolution. The degradation study was terminated after 3 months, after which the pH 10 buffer solutions containing dissolved hydrogel samples were freeze-dried and analysed using MALDI-ToF MS. Analysis of the acquired spectra of the degraded 6k hydrogel in Fig. 7b showed that the molecular weight of the residues of the degraded hydrogel was in accordance with that of unmodified PEG-6k. This supports the hypothesis that degradation occurred as a result of hydrolysis of the ester bonds in the structure, as this would mean cleavage of the G1-allyl end groups. The freeze-dried samples were furthermore analysed with NMR spectroscopy in the attempt of identifying formed degradation products. ^{1}H and ^{13}C NMR spectra (Fig. S1–S4 in the ESI†) indicated both trimethylol propane (TMP) **3** and compound **4** as products from the degradation, as suggested in Fig. 7c. Peaks characteristic to both **3** and **4** are present in the spectra whereas some peaks characteristic for the starting materials, TMP-$(SH)_3$ and PEG-G1-allyl, cannot be detected. This further supports the theory that the ester bonds in the hydrogels had been hydrolysed. The resolution of the spectra and the presence of many different compounds in the samples made it difficult to draw further conclusions about the degradation products. NMR spectra for PEG-6k-G1-allyl, TMP-(SH_3), TMP, and Na_2CO_3, as well as estimated NMR spectra for compound **4**, can be found in the ESI,† along with the NMR spectra for the degraded samples.

Conclusions

The purpose of this study was to gain a better understanding of the structure-to-property relationships of well-defined allyl-functional first-generation PEG hydrogels. The key to controlling the properties of hydrogels lies in controlling the network structure. Understanding the structure–property relationships and being able to control the final properties of the materials are essential for the development of hydrogels for applications in *e.g.* biomedicine.

The anhydride chemistry used in this work proved to be a facile approach for the functionalization of PEG materials, as shown by NMR, SEC and MALDI-ToF MS. Characterization of the thermal properties of synthesized PEG derivatives showed that replacing the hydroxyl end groups with G1-allyl reduced the crystallinity of the materials and also lowered the transition temperatures for both crystallization and melting. The differences between PEG-OH and PEG-G1-allyl in terms of thermal properties were additionally more pronounced at lower molecular weights.

Hydrogels were easily formed using thiol–ene coupling chemistry (TEC). TEC proved to be a robust strategy for the formation of well-defined crosslinked hydrogels with tunable properties. Networks formed from PEG-G1-allyl with higher molecular weights had a higher swelling degree, were more ductile and more susceptible to hydrolysis than networks formed from PEG-G1-allyl with lower molecular weights. By changing the molecular weight, hydrogels were produced with swelling ratios ranging from 240 to 1400% and Young's moduli ranging from 6 to 106 kPa. The molecular weight of the PEG chain was also found to greatly affect the degradation time in pH 10 buffer, where the time until complete dissolution into the medium ranged from 2 days to 5 weeks.

In summary, it has herein been shown that TEC is a powerful crosslinking strategy for the synthesis of well-defined network structures and that the properties of the final hydrogels can be easily tuned by varying the network constituents.

Acknowledgements

Wilhelm Beckers Jubileumsfond is acknowledged for financial support.

References

1 N. A. Peppas, J. Z. Hilt, A. Khademhosseini and R. Langer, *Adv. Mater.*, 2006, **18**, 1345–1360.
2 N. A. Peppas, K. B. Keys, M. Torres-Lugo and A. M. Lowman, *J. Controlled Release*, 1999, **62**, 81–87.
3 B. V. Slaughter, S. S. Khurshid, O. Z. Fisher, A. Khademhosseini and N. A. Peppas, *Adv Mater*, 2009, **21**, 3307–3329.
4 C. C. Lin and K. S. Anseth, *Pharm. Res.*, 2009, **26**, 631–643.
5 N. A. Peppas, Y. Huang, M. Torres-Lugo, J. H. Ward and J. Zhang, *Annu. Rev. Biomed. Eng.*, 2000, **2**, 9–29.
6 J. A. Burdick and K. S. Anseth, *Biomaterials*, 2002, **23**, 4315–4323.
7 A. M. Kloxin, A. M. Kasko, C. N. Salinas and K. S. Anseth, *Science*, 2009, **324**, 59–63.
8 C.-C. Lin, A. Raza and H. Shih, *Biomaterials*, 2011, **32**, 9685–9695.

9 M. Malkoch, R. Vestberg, N. Gupta, L. Mespouille, P. Dubois, A. F. Mason, J. L. Hedrick, Q. Liao, C. W. Frank, K. Kingsbury and C. J. Hawker, *Chem. Commun.*, 2006, 2774–2776.
10 W. H. Binder and R. Sachsenhofer, *Macromol. Rapid Commun.*, 2008, **29**, 952–981.
11 A. B. Lowe, *Polym. Chem.*, 2010, **1**, 17–36.
12 T. Yang, H. Long, M. Malkoch, E. K. Gamstedt, L. Berglund and A. Hult, *J. Polym. Sci., Part A: Polym. Chem.*, 2011, **49**, 4044–4054.
13 T. Yang, M. Malkoch and A. Hult, *J. Polym. Sci., Part A: Polym. Chem.*, 2013, **51**, 363–371.
14 T. Yang, M. Malkoch and A. Hult, *J. Polym. Sci., Part A: Polym. Chem.*, 2013, **51**, 1378–1386.
15 D. D. McKinnon, A. M. Kloxin and K. S. Anseth, *Biomater. Sci.*, 2013, **1**, 460–469.
16 M. W. Tibbitt and K. S. Anseth, *Biotechnol. Bioeng.*, 2009, **103**, 655–663.
17 M. I. Montanez, L. M. Campos, P. Antoni, Y. Hed, M. V. Walter, B. T. Krull, A. Khan, A. Hult, C. J. Hawker and M. Malkoch, *Macromolecules*, 2010, **43**, 6004–6013.
18 K. Oberg, Y. Hed, I. J. Rahmn, J. Kelly, P. Lowenhielm and M. Malkoch, *Chem. Commun.*, 2013, **49**, 6938–6940.
19 K. Olofsson, O. C. J. Andrén and M. Malkoch, *J. Appl. Polym. Sci.*, 2014, **131**, 39876.
20 H. Ihre, O. L. P. De Jesus and J. M. J. Frechet, *J. Am. Chem. Soc.*, 2001, **123**, 5908–5917.
21 G. Mun, I. Suleimenov, K. Park and H. Omidian, in *Biomedical Applications of Hydrogels Handbook*, Springer, New York, 2010, pp. 375–391.
22 N. A. Peppas and E. W. Merrill, *J. Appl. Polym. Sci.*, 1977, **21**, 1763–1770.
23 P. J. Flory, *Principles of Polymer Chemistry*, Cornell University Press, Ithaca, NY, USA, 1953.
24 D. W. van Krevelen and K. te Nijenhuis, *Properties of Polymers: Their Correlation with Chemical Structure; their Numerical Estimation and Prediction from Additive Group Contributions*, Elsevier Science Publishers B.V., Amsterdam, Netherlands, 3rd edn, 1990.
25 E. W. Merrill, K. A. Dennison and C. Sung, *Biomaterials*, 1993, **14**, 1117–1126.
26 N. Boucard, C. Viton and A. Domard, *Biomacromolecules*, 2005, **6**, 3227–3237.
27 L. G. Cima and S. T. Lopina, *Macromolecules*, 1995, **28**, 6787–6794.
28 L. Vervoort, I. Vinckier, P. Moldenaers, G. Van Den Mooter, P. Augustijns and R. Kinget, *J. Pharm. Sci.*, 1999, **88**, 209–214.
29 C. T. McKee, J. A. Last, P. Russell and C. J. Murphy, *Tissue Eng., Part B*, 2011, **17**, 155–164.
30 S. Mongkhontreerat, K. Oberg, L. Erixon, P. Lowenhielm, A. Hult and M. Malkoch, *J. Mater. Chem. A*, 2013, **1**, 13732–13737.
31 R. P. Schwarzenbach, P. M. Gschwend and D. M. Imboden, in *Environmental Organic Chemistry*, John Wiley & Sons, Inc., 2nd edn, 2003, pp. 513–535.
32 N. Feliu, M. V. Walter, M. I. Montanez, A. Kunzmann, A. Hult, A. Nystrom, M. Malkoch and B. Fadeel, *Biomaterials*, 2012, **33**, 1970–1981.